

Sentinel-2 based mapping of soil salinity of arid soils in southeastern regions of Tunisia

Sameh Hafra

University of Gabes Faculty of Sciences of Gabes: Universite de Gabes Faculte des Sciences de Gabes

Houda Sahnoun (✉ houdaenis@yahoo.fr)

University of Gabes Faculty of Sciences of Gabes: Universite de Gabes Faculte des Sciences de Gabes

Abbelhakim Bouajila

University of Gabes Faculty of Sciences of Gabes: Universite de Gabes Faculte des Sciences de Gabes

Research Article

Keywords: remote sensing, linear regression model, arid land, soil salinity

Posted Date: April 6th, 2022

DOI: <https://doi.org/10.21203/rs.3.rs-1511080/v1>

License: © ⓘ This work is licensed under a Creative Commons Attribution 4.0 International License.

[Read Full License](#)

Abstract

Arid and semi-arid regions are faced on soil salinization's problem causing land degradation that's why studies are focused on the prevention and the mitigation of this parameter in these environments. It degrades soil, limits plant growth and reduces crop productivity. Recently, the demand for rapid and economic detection of soil salinization has been rising. Remote sensing and multispectral data Sentinel_2 are used to predict and mapping soil salinity in southern Tunisia. In this study, 80 samples were collected from the soil surface (the upper 10 cm). A predictive model was constructed based on the measured soil electrical conductivity (EC) and spectral indices developed from satellite image. The results revealed that salinity index SI1, SI2 and band 3 have the highest correlation with EC. Multiple regression analysis showed a moderate accuracy with $R^2 = 0.42$ and an RMSE = 18.3.

This predictive model, special to arid and semi-arid environments, can be applied to other satellite data (Landsat 8...).

1. Introduction

Arid and semi-arid regions are characterized by low rainfall high evaporation, and restricted leaching. They are also characterized by degraded soils due to high salinity which decline soil quality and a lack of their fertility (Sidike et al., 2014; Makinde & Oyelade, 2019).

So the quality of soils of these regions mainly depends on the presence of the amount and types of salts such as anhydrite (CaSO_4), calcite (CaCO_3), gypsum ($\text{CaSO}_4 \cdot 2\text{H}_2\text{O}$), Halite (NaCl), and dolomite ($\text{CaMg}(\text{CO}_3)_2$).

Land degradation caused by soil salinity has been a global issue in dry regions (Qadir et al., 2006) either in Tunisia. However, more than 8% of the Tunisia surface is already affected by salinization to different degrees (Antipolis, 2003).

So it seems important to characterize and monitor the evolution of affected soils, in order to control the new saline distributions that these various interventions may induce and preserve these particularly sensitive environments from possible degradation.

The soil salinization is manifested as one of the main factors limiting the development of plants, reduction of arable land and degradation of soil quality by deteriorating the physico-chemical and biological properties of soil and groundwater, which threatens the "Food balance" mainly in arid to semi-arid regions.

However, the physico-chemical parameters of the soil are characterized by their evolution both in time and in space. This evolution of the landscape poses a large number of problems and difficulties for soil scientists in monitoring the parameters. But, the use of the traditional tools (laboratory analysis, field)

doesn't allow the monitoring of the speed of spatial and temporal evolution of this parameter causing the land degradation.

This has led us in recent years to explore more rapid and fairly reliable investigation methods such as spatial remote sensing which is of paramount importance for the mapping and monitoring of environmental problems. This approach, based on the study of natural surfaces by satellite images, through the intermediary of spectral surface properties, mainly linked to soil properties.

Remote sensing techniques using intelligent algorithms can predict surface salinity at various time intervals in large-scale regions (Metternicht & Zinck, 2003; Bouaziz et al., 2011; Sidike et al., 2014) such as artificial neural network (Seyam & Mogheir, 2011; Phonphan et al., 2014; Naderi et al., 2017; Ghimire et al., 2019; Li & Wang, 2019; Wang et al., 2018), classification and regression tree, fuzzy logic, Bayesian analysis, geostatistics, multivariate statistical technique (Principal Components Analysis (PCA), cluster analysis) (bouaziz et al., 2018), were studied to map soil salinity in the past decades (Hihi et al., 2019).

In southern Tunisia, many studies were developed. Bouaziz et al. (2018) showed that in the arid region we can apply the regression model because it is characterized by its efficiency and rapidity on predicting soil salinity. Hihi et al (2019), developed a multiple regression model relate electrical conductivity, sentinel_2 bands and salinity index. The objective of this study is to highlight the relationship between the results of soil analysis by traditional means (laboratory analysis) and those given from satellite images (spectral indices), in order to extract spatial variability of soil salinity in Tataouine region which is characterized as extremely arid zone, in the majority basins, the soils are covered by calcareous and / or gypsum crusts. So it's threatened by salinity.

2. Materials And Methods

2.1 Study area

The studied region of BeniBlel and Bessiouf watersheds was extending from longitudes 10°35'53.34"E and latitudes 32°52'14.31"N in Tatawin governorate (Fig. 1). It covers an area of 421 Km². The geological deposits are aged from Triassic and middle Jurassic (Chandoul et al., 1993).

Tataouine is located in the presaharian part of Tunisia (35°256' N, 10°227' E), which is a part of the Jeffara region. It is characterized by an arid climate; with a mean annual rainfall about 120 mm. And an annual average air temperature about 20.2°C. Were temperatures are high in summer and relatively low in winter.

In Tataouine governorate, soils are rich in salts such (as chlorides, sulphates and carbonates) which given place to a rare vegetation. Escadafal (1987) showed that soils are composed by calcareous loam, stones and crusts, red quartzic sand and gypsiferous crusts. Reliefs are dominated by tabular one and wide plains which are mainly used for extensive ranging.

2.2 Methodology

The methodology adopted in this study is based on two phases; the first one, data were collected. Actually, two groups of datasets were used; field measurements and spectral data obtained from satellite image (sentinel_2). In the second one, the calibration of general regression models from the analysis of these data was applied

2.3. Soil sampling

The soil samples were collected in June and July 2019 from total of 80 sites, within the upper 10cm from the soil surface. The choice of the sampling points does not respect a precise grid (Fig. 1), but it was based on many criteria such as the good distribution of the points in the study area, the variability of the soil types as well as the mode of occupation and accessibility of the land.

To locate the sampling points, we used a GPS (note that the geospatial reference system used is the UTM (Universal Transverse Mercator) in the WGS84 geodetic system North area 32).

Soil salinity is expressed as electrical conductivity (EC), which is measured using 1/5 soil/water diluted extracts.

2.4. Remote sensing data used

To predict soil salinity, we used the satellite image Sentinel-2 downloaded from the United States Geological Survey (USGS). This image was acquired in June 2019 in order to match the same date of soil sampling camping. Actually, in this period the arid regions are marked with a decrease in the vegetation cover, so the spectral signature measured from the soil can be badly recorded and must be adjusted (Palacios-Orueta et al., 1999; Bartholomeus et al., 2010). In addition, in this period, the signal of salty soil is easier to detect from the optical sensors (Dutkiewicz et al., 2009).

The sentinel-2 image is composed by 13 spectral bands which are represented by a spectrum of wave lengths varying from the blue band (443 nm) to the SWIR band (2190 nm). It is characterized also by a spatial resolution varying from 10 to 60 meters.

To predict soil salinity from satellite images, we based on the spectral response characteristics, because, saline soil are characterized by high reflection in the visible and near-infrared spectral (Gao et al., 2011).

Spectral analysis by means of radiometric indices is the classic and efficient method which allows giving exact descriptions of soil surface (Houssa, 1997). This lasts are calculated basing on different bands (blue, green, red and near infra-red). Therefore, 9 indices were examined in this study (Table 2).

Table 1
Pedological potentiel of Tataouine soil's

Fertility class	Area	%
Fertile	137412	28.8
Moderately fertile	139159	29.1
Not very fertile	70354	14.7
Very infertile	53742	11.3
Soil Complex : associations ranging from fertile to very fertile	73360	15.4
Urban	3429	0.7
Total	477456	100

Table 2
Indices formula used

Spectral indices	Equation	References
Brightness index	$BI = \frac{\sqrt{B^2 + G^2 + R^2}}{\sqrt{3}}$	Zhuo Luo et al. 2008
Color index	$CI = \frac{(R - G)}{(R + G)}$	Zhuo Luo et al 2008
Hue index	$HI = \frac{(2R - G - B)}{(G - B)}$	Zhuo Luo et al 2008
Redness index	$RI = \frac{R^2}{(B * G^3)}$	Zhuo Luo et al 2008
Salinity index 1	$SI = \sqrt{B * R}$	Khan et al 2005
Salinity index 2	$SI = \sqrt{G * R}$	Khan et al 2005
Salinity index 3	$SI = \sqrt{G^2 + R^2 + NIR^2}$	Douaoui et al 2006
Salinity index 4	$SI = \sqrt{G^2 + R^2}$	Douaoui et al 2006
Salinity index 9	$SI = \frac{NIR * R}{G}$	Abass et Khan 2007

2.5. Statistical analyses

After completing the collection of analytical data, and the data extracted from the satellite image, a linear regression model based on the Pearson correlation between spectral data and EC values obtained from laboratory was developed.

Globally, in studies used remote sensing in the monitoring of soil parameters, a linear regression was set between spectral indices and chemical properties measured in the laboratory (Baugh *et al.*, 1998; Crouvi & Ben-Dor, 2006). The multiple regression model is commonly used to correlate data and develop a model that could estimate soil salinity from spectral data (Albed *et al.*, 2013). In this work, we use the tool 'SPSS' for the statistical analysis.

The evaluation of the model performance is realized by the calculation of the coefficient of determination (R^2) and the root mean square error (RMSE) where;

R^2 is defined as the squared value of the correlation coefficient; it is a measure of the quality of the linear regression models; the highest values marked the optimal calibrated model. Although the smallest value of the root mean square error (Eq. 1) indicates the most accurate prediction.

$$\text{RMSE} = \sqrt{\frac{1}{N} \sum_{i=1}^N [Z^*(x_i) - Z(x_i)]^2} \quad (1)$$

Where:

N : Points number,

$Z^*(x_i)$ is the estimated value at point x_i

and $Z(x_i)$ is the observation value at point x_i .

3. Results

3.1. Soil properties

Based on soils analyses and according to Brown *et al.* (1954), soil salinity classification, the investigation area is considered as highly affected by salinity with basic pH value. It is characterized also by a gypsic soil and moderately high values of calcareous.

The granulometric analyses showed that the study area soils are mainly sandy to sandy loam.

The distribution of salinity, calcareous and gypsum values are shown in Fig. 2.

3.2. Statistical descriptive analyses

The experimental results indicate that the EC varies spatially around the medium (8.73 dS/m) significantly (Table 3). It deviates between 0.16 dS/m as a minimum and 103 dS /m as a maximum.

Table 3
Descriptive statistics on EC.

	Max	Min	Average
EC (dS/m)	103	0.16	8.73

3.3. Measured EC and spectral indices correlation

In this study, a correlation analyzes between the measured EC and the spectral indices proposed in Table 2 were carried out. These correlations are based on r of the Pearson function. The correlation between the EC and the spectral indices is given by Table 4. In absolute value, it is clear that the spectral indices most correlated with the EC values are the salinity index SI1 with ($|r| = 0.26$), and SI2 with ($|r| = 0.24$). Furthermore color indices are low correlated with the EC measured in the laboratory. Also, the sentinel-2 bands more correlated are band 2 and band 3 (Table 5).

Table 4
Correlation matrix between salinity indices and EC values

	EC	SI1	SI2	SI3	SI4	SI9	HI	CI	BI
EC	1								
SI1	0.26	1							
SI2	0.24	0.99	1						
SI3	0.23	0.96	0.97	1					
SI4	0.22	0.98	1.00	0.98	1				
SI9	0.10	0.74	0.79	0.88	0.83	1			
HI	-0.14	-0.14	-0.17	-0.14	-0.12	0.13	1		
CI	-0.12	0.33	0.39	0.46	0.46	0.78	0.50	1	
BI	0.23	0.99	1.00	0.98	1.00	0.79	-0.16	0.39	1

Table 5
Correlation matrix between sentinel-2 bands and EC values

	<i>CE</i>	<i>b4</i>	<i>b3</i>	<i>b2</i>	<i>b8</i>	<i>b11</i>	<i>b12</i>
CE	1						
b4	0.20	1					
b3	0.29	0.90	1				
b2	0.33	0.80	0.96	1			
b8	0.24	0.91	0.83	0.72	1		
b11	0.08	0.85	0.66	0.50	0.75	1	
b12	0.00	0.67	0.37	0.18	0.58	0.91	1

3.4. Quantitative mapping of soil salinity

Based on Sentinel-2 bands and the spectral indices, a multiple regression model was established (Table 6). This model is associated with the identification of 6 variables.

Table 6
Multiple regression model between spectral indices and measured EC

Regression model	R^2	RMSE
$EC = -109.92 - 0.1b4 + 0.08b2 - 0.03b3 - 0.03SI2 + 0.07b8 - 0.05b6 + 0.03SI1$	42%	18.3ds/m

The correlation curve between estimated and measured EC values shows that the values from ground truth are often higher than the estimated values (Fig. 3).

4. Discussion

From year to year, Soil salinity varied greatly, and being the important factor affecting plant growth especially in arid zone where second salinization occurred frequently also the pedological potential is very low. In this paper, soil salinity was investigated by linear regression model between EC value measured in the laboratory and salinity indexes extracted from Sentinel-2 image.

According to the results obtained, it can be said that the model is acceptable, having a coefficient of determination R^2 equal to 0.42. And a standard error RMSE is about 18.3 ds/m. This error is proportional to the salinity of the soil. Thus, to ensure the accuracy between the predicted conductivity and the ground truth measurement, it is necessary to have a low electrical conductivity.

This value suggests that the data fits the model well. Therefore, salinity can be mapped based on this model.

In the literature, several authors have worked on the theme dealt with in our work, and the results illustrate R^2 value differs from a study to another (Table 7). These studies showed that each region has its own models, and there is no specific index that can predict salinity in all regions. In fact the performance of each model is according to physical and environmental characteristics and the spatial extent of the study area.

Table 7
Examples of remote sensing applications for soil salinity prediction

Study area	R^2	Reference
France (Beauce)	0.4 0.82	Berthier et al, 2008
Iran (Urmia lake)	0.87	Rahmati and Hamzhepour, 2017
USA (north Carolina)	0.54 0.67	Davis et al, 2019
Abu Dhabi, United Arab Emirates	0.71	Abuelgasim and ammad, 2019
Cairo Egypt	0.94	Morgan et al, 2018
Tunisia (Gabes-Ghannouch)	0.48	Hihi et al, 2019
Tunisia (Gabes-Ghannouch)	0.72	Bouaziz et al, 2018

5. Conclusion

This study is interested in the estimation of soil salinity by remote sensing in the region of Tataouine. The estimation of soil salinity is carried out through the calibration of a regression model relate the salinity indexes extracted from Sentinel-2 image and EC values from grand truth. This model is validate with a coefficient of determination $R^2 = 42\%$.

This current study and other similar case studies showed that it is possible to detect soil salinity and quantitatively estimate its spatial distribution, thanks to this regression equation.

The advantage of this method is that it saves a lot of time and is less expensive, since the large evolution of soil salinity both in time and in space. Conversely, the disadvantage of this approach lies in the low precision, compared to conventional laboratory analyzes associated with specific sites.

It is therefore clear that remote sensing is useful in determining soil salinity, that is why the scientific community should move on to using this tool not only to predict salinity, but also we can apply this method in the monitoring of soil organic matter (Wang et al., 2018), gypsum content, soil texture (Shahriari et al., 2019), soil total nitrogen (Zhang et al., 2019), and clay (Paul et al., 2020)...

Declarations

No Conflicts of interests.

Statements

If we consider all the knowledge obtained on this subject, it is clear that the scientific community should use remote sensing, develop this tool and determine standards and models (for each region) for predicting physico-chemical parameters of the soil such salinity.

The traditional ways of sampling and routine soil analyses are expensive especially in the case of graet areas, so, through this work we learned that the mapping of perennial soil prooporties obtained by remote sensing is not only a product and therefore an end but can in turn become “basic data”.

References

1. Abbas A, Khan S (2007) Using remote sensing techniques for appraisal of irrigated soil salinity. In Proceedings of the International Congress on Modelling and Simulation (MODSIM'07), 2632–2638, Modelling and Simulation Society of Australia and New Zealand, Brighton, UK
2. Abuelgasim A, Ammad R (2019) Mapping soil salinity in arid and semi-arid regions using Landsat-8 OLI satellite data. *Remote Sens Appl: Soc Environ* 13:415–425 <https://doi.org/10.1016/j.rsase.2018.12.010>
3. Allbed A, Kumar L (2013) Soil salinity mapping and monitoring in arid and semi-arid regions using remote sensing technology: a review. *Adv Remote Sens* 2(4):373–385 DOI: 10.4236/ars.2013.24040
4. Allison LE, Bernstein L, Bower CA, Brown JW, Fireman M, Hatcher JT, Hayward HE, Pearson GA, Reeve RC, Richards A, Wilcox LV (1954) *Diagnosis and Improvement of Saline and Alkali Soils*. United States Department of Agriculture, Agriculture Handbook, vol 60. Soil and Water Conservation Research Branch Agricultural Research Service
5. Antipolis S (2003) *Les menaces sur les sols dans les pays méditerranéens. Plan bleu pour la méditerranée*
6. Bartholomeus HM, Schaepman ME, Stevens A, Hoogmoed WB, Spaargaren OSP (2008) Spectral reflectance based indices for soil organic carbon quantification. *Geoderma* 145:28–36 [doi:10.1016/j.geoderma.2008.01.010](https://doi.org/10.1016/j.geoderma.2008.01.010)
7. Baugh W, Kruse FA (1998) Quantitative geochemical mapping of ammonium minerals in the southern Cedar Mountains, Nevada, using the AVIRIS. *Remote Sens Environ* 65(3):292–308 [https://doi.org/10.1016/S0034-4257\(98\)00039-X](https://doi.org/10.1016/S0034-4257(98)00039-X)
8. Berthier L, Pitres JC, Vaudour E (2008) Prédiction spatiale des teneurs en carbone organique des sols par spectroscopie de terrain visible-proche infrarouge et imagerie satellitale SPOT - Exemple au niveau d'un périmètre d'alimentation en eau potable en Beauce. *Etude et Gestion des Sols* 15(4):213–224
9. Bouaziz M, Chtourou MY, Triki I, Mezner S, Bouaziz S (2018) Prediction of soil salinity using multivariate statistical techniques and remote sensing tools. *Adv Remote Sens* 7(4):313–326 [doi:10.4236/ars.2018.74021](https://doi.org/10.4236/ars.2018.74021)

10. Bouaziz M, Matschullat J, Gloaguen R (2011) Improved remote sensing detection of soil salinity from a semi-arid climate in Northeast Brazil. *Comptes Rendus Geosci* 343:795–803 <https://doi.org/10.1016/j.crte.2011.09.003>
11. Chandoul H, Burrolet PF, Ben Ferjani A, Memmi L (1993) *Recueil des coupes Types de Tunisie: Trias et Jurassique*. Mémoire n° 4, E.T.A.P, 95 p
12. Crouvi O, Ben-Dor E, Beyth M, Avigad D, Amit R (2006) Quantitative mapping of arid alluvial fan surfaces using field spectrometer and hyperspectral remote sensing. *Remote Sens of Environ* 104(1):103–117 DOI: 10.1016/j.rse.2006.05.004
13. Davis E, Wang C, Dow K (2019) Comparing Sentinel-2 MSI and Landsat-8 OLI in soil salinity detection: a case study of agricultural lands in coastal North Carolina. *Int J of Remote Sens* 40(16):6134–6153 <https://doi.org/10.1080/01431161.2019.1587205>
14. Douaoui AEK, Nicolas H, Walter C (2006) Detecting Salinity Hazards within a Semiarid Context by Means of Combining Soil and Remote-Sensing Data. *Geoderma* 134:217–230 [10.1016/j.geoderma.2005.10.009](https://doi.org/10.1016/j.geoderma.2005.10.009)
15. Dutkiewicz A, Lewis M, Ostendorf B (2009) Evaluation and Comparison of Hyperspectral Imagery for Mapping Surface Symptoms of Dry Land Salinity. *Int J of Remote Sens* 30(3):693–719 <https://doi.org/10.1080/01431160802392612>
16. Escadafal R (1987) Soil scientist in agricultural ministry, Tunisia. *Carte des ressources en sols de la Tunisie feuille de Tataouine*
17. Gao F, Huang Q, SUN X, Yan Z (2011)) Study on Dynamic Changes of the Soil Salinization in the Upper Stream of the Tarim River Based On RS and GIS. *Proced Environ Sci* 11:1135–1141. DOI: 10.1016/j.proenv.2011.12.171
18. Ghimire S, Deo RC, Raj N, Mi J (2019)) Wavelet-based 3-phase hybrid SVR model trained with satellite-derived predictors, particle swarm optimization and maximum overlap discrete wavelet transform for solar radiation prediction. *Renew and Sustain Energy Rev* 113:109–247 Doi: 10.1016/j.rser. 2019.109247
19. Hihi S, Bouaziz M, Ben-Rabah Z, Chtourou MM (2019) Prediction of soil salinity using remote sensing tools and linear regression model. *Advanc in Remote Sens* 8(3):77–88 DOI: 10.4236/ars.2019.83005
20. Houssa R (1996) *Etude radiométrique des sols d'une zone sahélienne (programme Hapex-Sahel): analyse multi-échelle : du laboratoire au satellite*. Paris : ORSTOM, 226 p. (Thèses et Documents Microfichés ; 161). Th. Géosci. : Géol. - Télédétection, ULP : Strasbourg. ISBN 2-7099-1344-5. ISSN 0767-922X.
21. Khan NM, Rastoskuev VV, Sato Y, Shiozawa S (2005) Assessment of hydrosaline land degradation by using a simple approach of remote sensing indicators. *Agric Water Manag* 77(1–3):96–109 DOI: 10.1016/j.agwat.2004.09.038
22. Li M, Wang H (2019) Development of ANN-GA program for back calculation of pavement moduli under FWD testing with visco elastic and nonlinear parameters. *Int J Pavement Eng* 20(4):490–498 <https://doi.org/10.1080/10298436.2017.1309197>

23. Makinde EO, Oyelade EO (2019) Land cover mapping using Sentinel-1 SAR and Landsat 8 imageries of Lagos State for 2017. *Environ Sci Pollut Res* 27:66–74 <https://doi.org/10.1007/s11356-019-05589-x>
24. Metternicht G, Zinck J (2003) Remote sensing of soil salinity: potentials and constraints. *Remote Sens Environ* 85(1):1–20 DOI: 10.1016/S0034-4257(02)00188-8
25. Morgan RS, El-Hady MA, Rahim IS (2018) Soil salinity mapping utilizing sentinel-2 and neural networks. *Indian J Agric Res* 52(5):524–529 DOI: 10.18805/IJARE.A-316
26. Naderi A, Delavar MA, Kaboudin B, Askari MS (2017) Assessment of spatial distribution of soil heavy metals using ANN-GA, MSLR and satellite imagery. *Environ Monit Assess* 189(5):214 DOI: 10.1007/s10661-017-5821-x
27. Palacios-Orueta A, Pinzón JE, Ustin SL, Roberts DA (1999) Remote Sensing of Soils in the Santa Monica Mountains: II. Hierarchical Foreground and Background Analysis. *Remote Sens Environ* 68(2):138–151 1016/S0034-4257(98)00106-0
28. Paul SS, Coops N, Johnson MS, Krzic M (2020) Mapping soil organic carbon and clay using remote sensing to predict soil workability for enhanced climate change adaptation. *Geoderma* 363 <https://doi.org/10.1016/j.geoderma.2020.114177>
29. Phonphan W, Tripathi NK, Tipdecho T, Eiumnoh A (2014) Modelling electrical conductivity of soil from backscattering coefficient of microwave remotely sensed data using artificial neural network. *Geocarto Int* 29(8):842–859 <https://doi.org/10.1080/10106049.2013.868040>
30. Qadir M, Noble AD, Schubert S, Thomas RJ, Arslan A (2006) Sodicty-induced land degradation and its sustainable management: problems and prospects. *Land Degrad Dev* 17(6):661–676 <https://doi.org/10.1002/ldr.751>
31. Rahmati M, Hamzhepour N (2017)) Quantitative remote sensing of soil electrical conductivity using ETM + and ground measured data. *Int J Remote Sens* 38(1):123–140 <https://doi.org/10.1080/01431161.2016.1259681>
32. Seyam M, Mogheir Y (2011) Application of artificial neural networks model as analytical tool for groundwater salinity. *J Environ Protect* 2(1):56 DOI: 10.4236/jep.2011.21006
33. Shahriari M, Delbari M, Afrasiab P, Pahlavan-Rad MR (2019) Predicting regional spatial distribution of soil texture in floodplains using remote sensing data: A case of southeastern Iran. *CATENA* 182(35):104–149 DOI: 10.1016/j.catena.2019.104149
34. Sidike A, Zhao S, Wen Y (2014) Estimating soil salinity in Pingluo County of China using QuickBird data and soil reflectance spectra. *Int J Appl Earth Obs Geoinform* 26:156–175 DOI: 10.1016/j.jag.2013.06.002
35. Wang B, Waters C, Orgill S, Gray J, Cowie A, Clark A, Li liu D (2018) High resolution mapping of soil organic carbon stocks using remote sensing variables in the semi-arid rangelands of eastern Australia. *Sci Tot Environ* 630:367–378 DOI:10.1016/j.scitotenv.2018.02.204
36. Zhang Y, Sui B, Ouyang L, Shen H (2019) Mapping stocks of soil total nitrogen using remote sensing data: A comparison of random forest models with different predictors. *Comput Electron Agric*

37. Zhuo L, Yaolin L, Jie C, Changji H (2008) JianW Quantitative retrieving of soil organic matter using field spectrometer and hyperspectral remote sensing, Proc. SPIE 7285. International Conference on Earth Observation Data Processing and Analysis (ICEODPA), 72850A

Figures

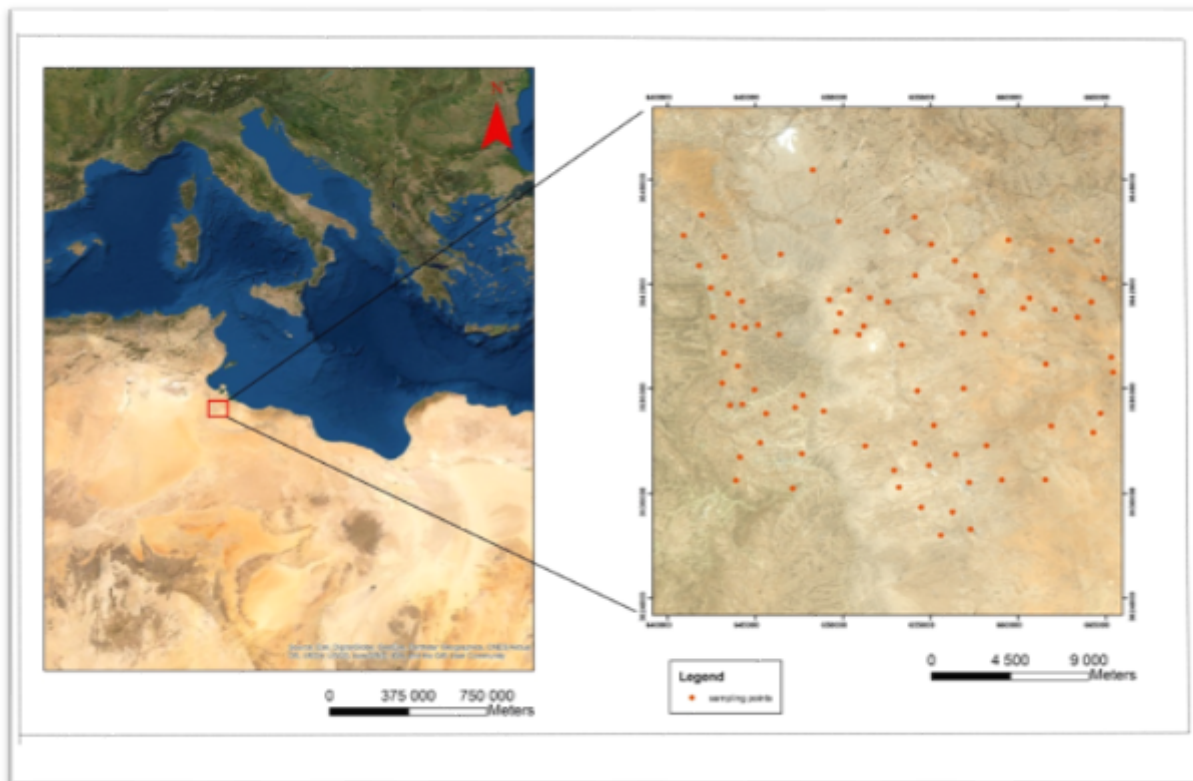


Figure 1

Study area and sampling location

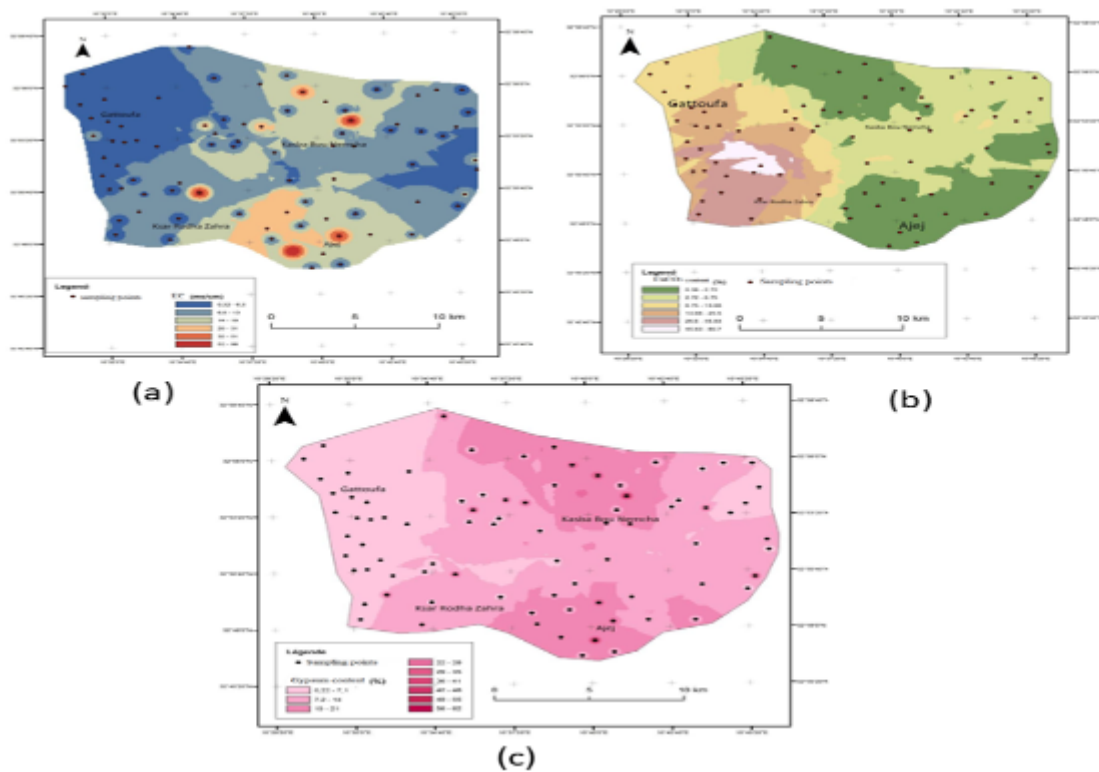


Figure 2

Spatial distribution of soil properties: (a) Spatial distribution of electrical conductivity values; (b) Spatial distribution of limestone content; (c) Spatial distribution of gypsum content

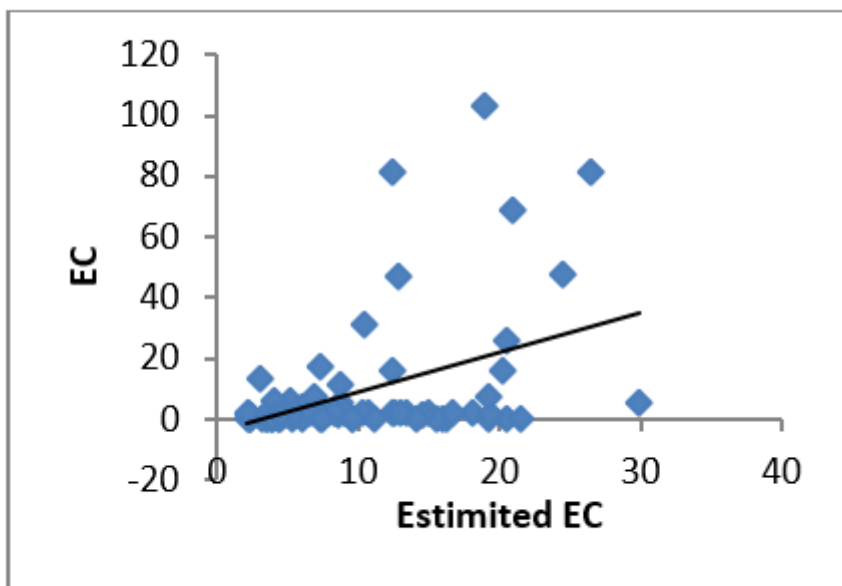


Figure 3

Correlation curve between estimated and measured EC